Evaporation Rates of Liquids to Flowing Gas Streams

D. E. SEVERSON, A. J. MADDEN, and EDGAR L. PIRET

University of Minnesota, Minneapolis, Minnesota

The influence of high concentration gradients and high evaporative velocities on rates of mass transfer was studied by evaporating liquids into low-speed inert gas streams at pressures approaching the vapor pressure of the liquids.

Inert gas concentration in some experiments changed nearly fivefold across the boundary layer. The velocity normal to the surface (owing to evaporation), usually neglected in comparison with main-stream velocity, varied from 0.038 to 19 times the main-stream velocity.

The data for air-water, air–carbon tetrachloride, air-chlorobenzene, and helium-chlorobenzene systems were represented within experimental error over the Graetz number range of 0.1 to 1,800 by the flat-duct equations of Butler and Plewes (*2*) and also by the usual dimensionless plots.

The influenee of high concentration gradients on the rates of mass transfer from evaporating liquids is of considerable interest to chemical engineering practice and has been much speculated upon (*12*). Presented herein are experimental data on the evaporation rates of several liquids into low-velocity gas streams over such a wide range of absolute pressures and flow rates, that the partial pressure of the nondiffusing component varied as much as fivefold within the boundary layer. By using subatmospheric pressures only slightly above the vapor pressures of the vaporizing liquids one could obtain high diffusivities and high evaporation velocities normal to the surface as compared to the main-stream velocities. Also, for example, the Schmidt number varied by a factor as high as 35 between surface and bulk-gas properties.

The data were computed in terms of several available equations; among these the equation of Butler and Plewes (*2*) was found to correlate the data within experimental accuracy over a range of Graetz numbers from 0.1 to 1,800 for diverse systems. Correlations were also obtained by plotting the Sherwood, Schmidt, and Reynolds number groups.

The importance to the rate of evaporation of the flow of heat through the liquid to its surface is underscored by the examination of a temperature profile for a particular run (Figure 1). In this case a temperature gradient of about 3.9°C./mm. of depth in the liquid was obtained. A 0.3-mm.–diameter thermistor was used to measure the temperature of the evaporating surface in all runs.

Data on the effect of concentration levels on mass transfer rates in the high Reynolds number range of 600 to 15,000 have been presented by Westkaemper and White (*13*) and Cairns and Roper (*3*).

EVAPORATION-RATE MEASUREMENTS

Scope

The liquid was evaporated from the open end of a 13-mm. O.D., 10.5-mm. I.D. vertical glass tube projecting into a 26.4-mm. I.D. horizontal round glass tube through which the inert gas was caused to flow at various rates and total pressures. The evaporation rate was determined by keeping the liquid surface level with the top of the vertical tube and measuring at various times the volume of liquid remaining in the supply tubing.

The systems studied were air-water, air–carbon tetrachloride, air-chlorobenzene, and helium-chlorobenzene. In addition, a few points were determined for helium-water and air-bromobenzene. Four measurements of the rates of evaporation of water into air from a 1.37- by 1.37-cm.–square surface, set flush with the bottom of a 2.54-by 2.54-cm.–square duct are also reported.

Total pressures ranging from 15 to 700 mm. Hg and average inert-gas flow velocities of 0.013 to 58 cm./sec. were used. Since all determinations were made at room temperature and all entering gas streams contained pure inert gas, variations in relative vapor concentration were attained by varying the total pressure and by studying several systems.

In most cases operation was adiabatic; that is, the room temperature was controlled at a constant value and the liquid surface, initially at room temperature, was allowed to approach a steady state temperature resulting from the evaporation regime. The surface temperature of the evaporating liquid was determined with a calibrated thermistor, 0.3 mm. in diameter, located just under and practically in contact with the under side of the evaporating surface.

The experimental arrangement of a cylinder projecting into a circular tube is perhaps not the simplest case for fluid-dynamics analysis. It was arrived at, after several other designs had been attempted, as convenient for this investigation, the objective of which was to investigate primarily from an experimental viewpoint the effect of high ratios of vapor to inert gas and the effect of high gradients on mass transfer rates.

Rate-Measuring System

A flow diagram of the experimental apparatus is shown in Figure 2. The evaporation section, consisting of a vertical tube the open end of which projected into a larger horizontal tube serving as the gas duct, may be seen in Figures 3 and 4.

D. E. Severson is at the University of North Dakota, Grand Forks, North Dakota, and Edgar L. Piret is at the American Embassy, Paris, France.

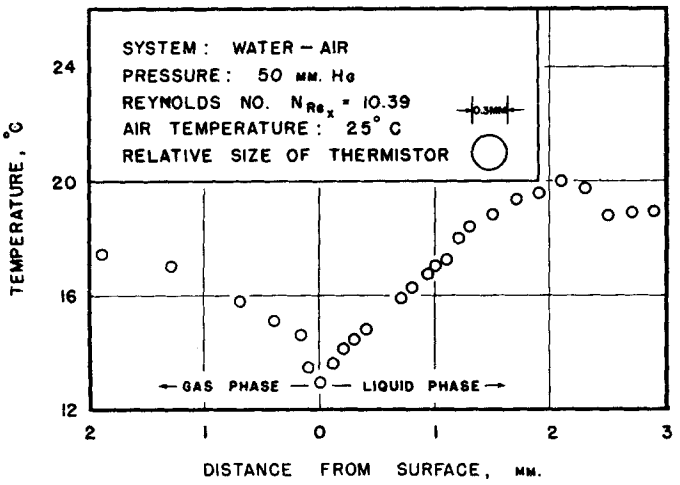

Fig. 1. Gas- and liquid-temperature profiles for an air-water run showing high gradients encountered.

These are photographs of evaporation in progress of titanium tetrachloride liquid into moist air. The evaporation section was built of Pyrex glass to facilitate cleaning and to permit observation of the progress of the evaporation. The square-duct experiments were made in a similar apparatus.

Evaporation rates were determined by measuring the time rate of change in the volume of the liquid supply contained in a *U* tube. The liquid was held in position by a column of mercury open on its other side to the atmosphere. The positions of the mercury-evaporating liquid meniscus and thus of the evaporating surface were adjusted first by the addition of mercury to the open end of the *U* tube and during a run by raising or lowering a glass rod. This rod extended into the mercury on the atmospheric side of the *U* tube and was moved by means of a screw-gear mechanism. During runs adjustments were made at frequent intervals to maintain the evaporating surface flat across the opening of the vertical tube. Timed observations of the position of the mercury-evaporating liquid meniscus with a cathetometer gave the evaporation-rate data.

It was found in a series of experiments that a change of 0.3 mm. in the position of the meniscus either above or below the flat surface of the glass tube changed the evaporation rate 2 or 3%.

The inert-gas flow rate was measured with a wet-test gas meter and the system operating pressure determined with a Zimmerli gauge or with a mercury manometer open to the atmosphere.

On the high-pressure side of the system (Figure 2) the gas train consisted of a wet-test meter, a capillary flow meter equipped with a water manometer, followed by desiccants silica gel, drierite, and calcium chloride, and a cotton-filled tube for removal of entrained dust. Reduction to operating pressure was made by a needle valve. A horizontal, round Pyrex tube of 2.64-cm. I.D. formed a calming section 70 cm. long preceding the evaporating surface, that is the flat, open end of a vertical Pyrex tube of 1.05-cm. I.D. and 1.30-cm. O.D. A needle-valve control was located following a 24-cm. length of the same-diameter tubing and a shorter constricted length. This in turn was followed by a 4-ft. vertical section of 2-in. standard pipe serving as a surge volume and finally by a vacuum pump. A bleeder-valve opening to the atmosphere was attached to the upper end of the 2-in. pipe to permit independent adjustment of flow rate and system pressure. The vertical evaporator tube projected into the horizontal tube at about 0.4 cm. below the center line (Figures 3 and 4).

Rate-Determination Procedure

Mercury was placed in the *U* tube (Figure 2), and the system was evacuated to a pressure below that at which the run was to be made. The liquid to be evaporated, having first been purged of dissolved air by boiling, was drawn into the system above the mercury through the sidearm filling tube. Final adjustments of the flow rate and system pressure to desired run conditions were made, and the liquid level was brought up to the level of the flat surface by the addition of more mercury to the *U* tube. A precise setting of the liquid level at the flat surface was made by adjustment of the glass rod. The time was recorded and the position of the mercury-evaporating liquid meniscus read with a cathetometer.

Evaporation was then allowed to proceed for a time interval which depended upon the rate for the particular run and varied from 30 sec. to 10 min. The level was then adjusted precisely to the original position by again lowering the glass rod by means of the screw mechanism. The new position of the mercury-liquid meniscus was noted. The volume of liquid evaporated during the time interval was equal to the tube volume displaced. This procedure was continued until enough observations had been made to establish the evaporation rate, the necessary run time being from 15 min. up to about 4 hr.

Following each cathetometer reading the evaporation surface temperature was measured with the calibrated 0.3-mm.-diameter spheroidal glass-coated bead thermistor, with a temperature coefficient of resistance of about 3.4%/°C. Since the thermistor reading depended upon the current flow, all readings were made with a potentiometer at a standard thermistor current of 10 μa. The thermistor was placed so that the bead tangentially just touched the under surface of the liquid when the liquid surface was flat across the opening.

During each run intermittent readings were taken of the wet-test meter, capillary flow manometer, meter thermometer, room thermometer, barometer, and system pressure gauge.

One of the major experimental difficulties encountered was in the release of dissolved gases by the evaporating liquid during the course of the measurement. To avoid this liquid was boiled several minutes to remove dissolved gases and taken up into a 50-cc. hypodermic syringe. The syringe needle was thrust into a cork and the liquid cooled in the syringe under the pressure of the weight of the plunger, thus preventing dissolution of air before introduction into the system under vacuum. The sidearm was first filled with gas-free liquid, the cork inserted into the flanged opening, and the liquid admitted slowly through the needle and stopcock.

Because of the tendency for organic compounds to accumulate at the surface of an immiscible liquid and markedly to affect evaporation rates, it was also essential to use great care to minimize contact between the stopcock lubricants and the liquid to be evaporated, especially in the runs with water.

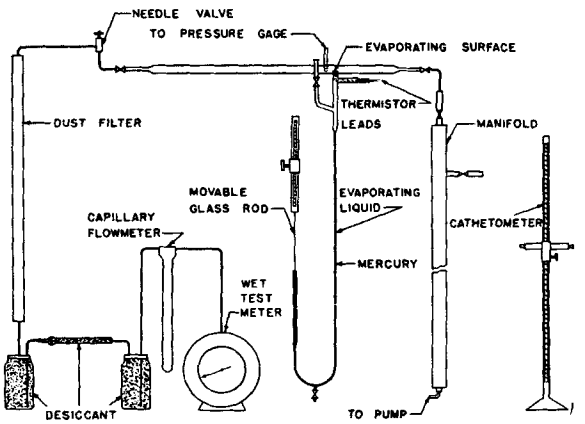

Fig. 2. Flow diagram of apparatus.

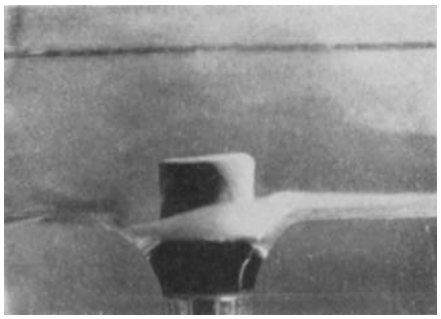

Fig. 3. Evaporation pattern of titanium tetrachloride into a stream of moist air; scale 4:3; data: p_T = 686 mm. Hg, N_{Re_z} = 66.8, $1/\psi$ = 958, v_n/u_0 (estimated) = 0.070.

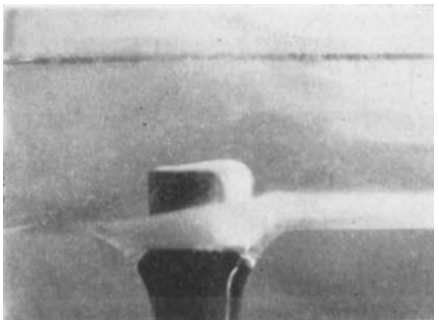

Fig. 4. Evaporation pattern of titanium tetrachloride into a stream of moist air; scale 4:3; data: p_T = 508 mm. Hg, N_{Re_z} = 58.7, $1/\psi$ = 840, v_n/u_0 (estimated) = 0.075.

High-vacuum silicone grease was found to be sufficiently insoluble for stopcock sealing purposes during runs.

Surface Temperature Important

The over-all mass transfer rate is highly dependent on the liquid surface temperature, since this determines the vapor pressure of the liquid at the interface and hence the driving force for evaporation. The surface temperature in turn depends on the evaporation rate and also upon the heat flow to the surface from the gas and liquid phases.

The magnitude of the temperature gradient near the evaporating surface is illustrated by the data of Figure 1. In this experiment the rigid thermistor connections were removed and the leads brought into the system through a flexible rubber tube. This permitted positioning the thermistor at various distances from the evaporating surface. The evaporation rate could not be measured simultaneously with the temperature profile in this experiment because the system volume was no longer rigid enough with the rubber connections to permit accurate measurement of the liquid volume change.

The temperature profile of Figure 1 was determined with evaporation proceeding under the conditions of run 88 (air-water at 50 mm. Hg). The very high temperature gradients through both gas and liquid films are to be noted, the liquid film gradient being 3.9°C./mm. of depth. By far the greater portion of the heat of vaporization in this run was transferred through the liquid film.

This extremely large temperature gradient in the liquid phase showed the necessity of very careful measurement of the surface temperature in evaporative runs to determine accurately the vapor pressure of the liquid at the surface where the evaporation occurs. Hence in evaporative-rate determinations the thermistor was placed as close to the surface as possible without its actually distorting the surface. This was accomplished by bringing the surface level to a point where the thermistor touched its reflection in the under surface of the liquid at each level adjustment. The thermistor was so placed in the system that the meniscus was flat across the opening after this adjustment had been made.

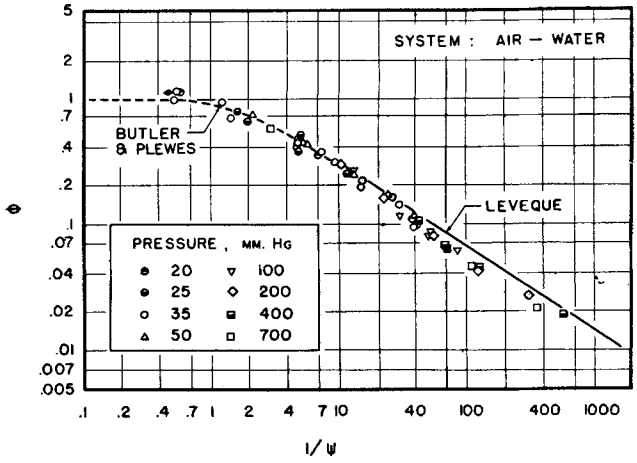

Fig. 6. Experimental mass transfer data for system air-water.

Practical utilization of any mass transfer correlation demands an accurate knowledge of the heat transfer situation as well as the flow situation. As a further illustration of the importance of this point, the results of runs 119 and 120 may be considered; both were made with air-water at 35 mm. total pressure, flow rates differing by less than 3%, and ambient air temperature 25°C. Run 119 was made in the usual manner, the surface being allowed to approach a steady state temperature which as measured with the thermistor averaged 14.7°C. Run 120 differed from 119 only in that additional heat was supplied to the surface by radiation from a hot chromel resistance wire suspended above the evaporating surface by means of a conical reflector. In this run the steady state temperature was 20.3°C. The

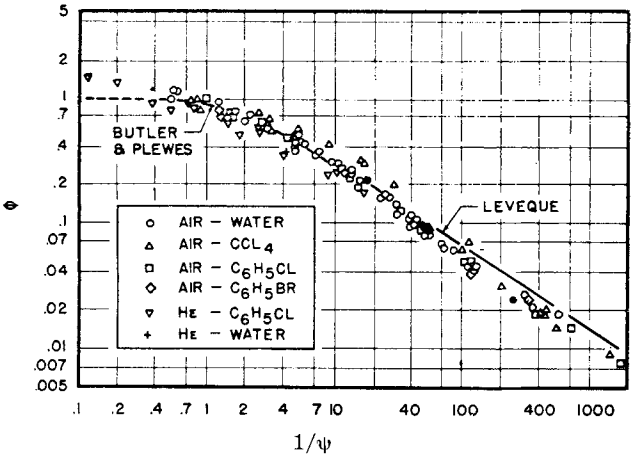

Fig. 5. Experimental mass transfer data for all systems studied; fractional saturation plotted vs. the Graetz number, curves calculated from Butler and Plewes's equations.

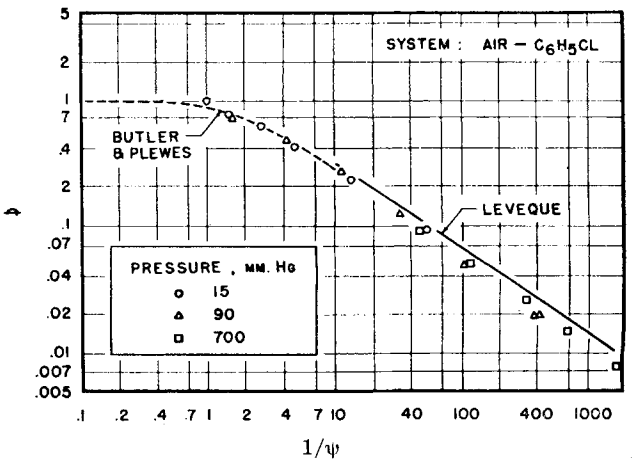

Fig. 7. Experimental mass transfer data for system air-chlorobenzene.

TABLE 1. SUMMARY OF EXPERIMENTAL DATA

Run number	System pressure p_T, mm. Hg	Temperature, gas t_o, °C.	Temperature, surface t_s, °C.	Vapor pressure P^*, mm. at surf.	Dry-gas rate, S.T.P. cu. ft./hr.	Evaporation rate, lb./ sq. ft./hr.	ϕ	$1/\psi$	v_n/u_o	$\frac{p_{Bo}}{p_{Bs}}$
System: Air-water.										
120	35.1	25.1	22.4	20.3	0.0136	1.55	1.17	0.543	17.8	2.37
119	35.0	25.1	17.1	14.7	0.0140	0.686	1.14	0.561	10.7	1.72
114	35.1	25.0	12.3	10.7	0.960	1.94	0.118	39.2	0.590	1.42
88	50.0	25.0	15.2	13.0	0.959	1.64	0.119	38.5	0.603	1.351
64	197.0	21.8	18.4	15.8	0.254	0.336	0.298	10.2	1.49	1.087
94	198.0	25.1	17.1	14.6	7.66	0.840	0.0276	307.	0.137	1.080
92	699.3	25.0	24.7	23.3	0.0748	0.0804	0.586	2.97	2.86	1.034
93	702.6	25.0	23.1	21.2	8.80	0.304	0.0213	350.	0.104	1.031
*SD5	187.	25.1	19.4	16.9	2.08	0.458	0.0971	50.1	0.339	1.10
*SD4	330.	25.0	20.9	18.5	0.765	0.218	0.201	18.5	0.703	1.06
*SD3	331.	25.0	20.5	18.1	11.7	0.407	0.0255	284.	0.0877	1.06
System: Air-chlorobenzene.										
153	15.0	25.0	21.4	9.48	0.00503	2.74	0.980	0.697	12.6	2.72
125	15.0	25.0	14.5	6.38	0.378	5.34	0.0947	52.9	0.487	1.74
141	90.0	25.1	23.4	10.6	0.236	1.15	0.121	32.6	0.608	1.13
145	700.	25.1	25.1	11.7	0.350	0.179	0.0903	48.5	0.447	1.017
143	700.	25.0	24.0	11.0	13.2	0.550	0.00787	1813.	0.0388	1.016
System: Air-carbon tetrachloride.										
166	120.	25.1	21.1	95.8	0.00639	5.45	0.816	0.885	11.4	4.96
157	118.	24.9	15.5	73.6	4.08	16.8	0.0142	571.	0.0707	2.66
123	200.	25.0	15.3	72.8	0.113	7.10	0.330	15.8	1.85	1.57
165	700.	25.0	24.6	113.	0.00602	0.505	0.960	0.829	5.57	1.19
159	700.	25.1	22.3	101.	10.4	6.19	0.00898	1440.	0.0442	1.17
System: Helium-chlorobenzene.										
186	15.0	25.0	18.6	8.09	0.0114	3.65	0.903	0.359	8.65	2.17
181	15.4	25.0	11.6	5.36	0.276	8.70	0.247	8.73	1.33	1.53
174	90.0	25.0	24.3	11.2	0.00373	0.283	1.48	0.116	8.91	1.14
175	696.	25.0	24.1	11.1	0.529	0.479	0.169	16.5	0.840	1.016
176	699.	25.1	23.9	11.0	1.71	0.680	0.0754	53.2	0.371	1.016
System: Air-bromobenzene.										
133	15.0	25.0	21.8	3.48	0.342	3.46	0.0911	50.4	0.461	1.30
136	35.0	25.0	24.1	4.01	0.00856	0.399	0.788	1.25	4.27	1.13
132	99.2	25.1	23.7	3.90	2.24	0.978	0.0236	329.	1.17	1.041
System: Helium-water.										
90	35.1	25.0	11.6	10.2	0.359	2.23	0.354	4.15	1.96	1.49

*Square duct runs

measured evaporation rate was 2.25 times as large in run 120 as in run 119, but the value of ϕ obtained was only 1.025 times as large showing that within experimental error the correlation of Figure 5 was equally valid for both runs.

Flow-Pattern Photographs

Because of the geometry used it was desirable to observe experimentally whether or not the evaporation pattern appeared undisturbed over the entire length of the cylinder. For this purpose liquid titanium tetrachloride was evaporated into moist air. The vapor pressure is comparable to that of chlorobenzene, and vapor densities are of the order of some of the systems studied. At the boundary layer a dense smoke was produced by the interaction of titanium tetrachloride and water, and the over-all shape of the boundary layer could be seen.

The photographs of Figures 3 and 4 show the visible boundary layer for the evaporation of titanium tetrachloride into streams of moist air at near-atmospheric pressure and at two air-flow rates near the high end of the range covered in the rate measurement runs. Even at these higher velocities, where separation or disturbance in the flow pattern might occur, the shape of the boundary layer appeared to be smooth and unbroken over the entire length of the evaporating surface. The calculated Reynolds numbers for all runs in the investigation are of course very low.

Visual observations of the titanium tetrachloride evaporation at lower flow rates, where the smoke was not dense enough to be photographed, also showed no evidence of tripping into turbulence along the evaporating surface.

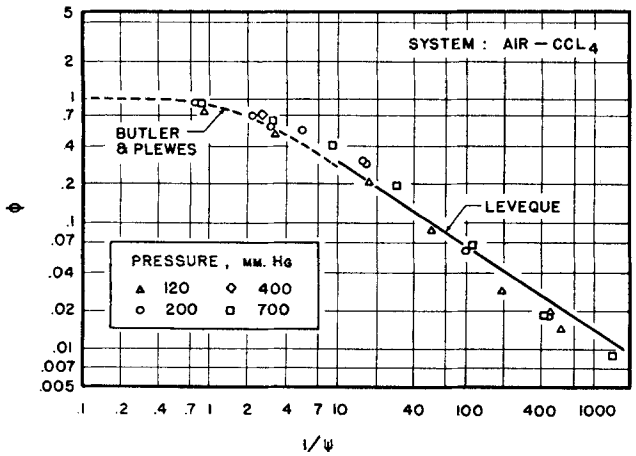

Fig. 8. Experimental mass transfer data for system air-carbon tetrachloride.

EXPERIMENTAL RESULTS

Representative data are summarized in Table 1*. Among the dimensionless groups calculated are the fractional saturation of the gas stream leaving the

*Tabular material has been deposited as document No. 5975 with the American Documentation Institute, Photoduplication Service, Library of Congress, Washington 25, D. C., and may be obtained for $2.50 for photoprints or $1.75 for 35-mm. microfilm

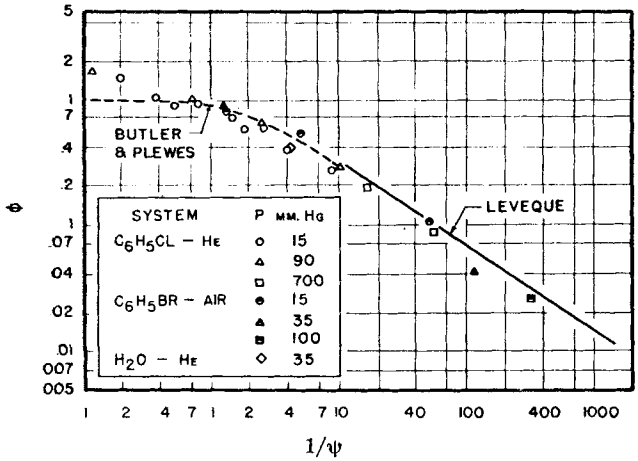

Fig. 9. Experimental mass transfer data for systems helium-chlorobenzene, air-bromobenzene, and helium-water.

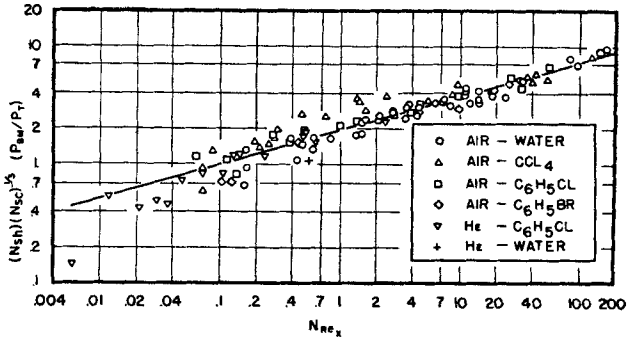

Fig. 10. Sherwood-Schmidt-Reynolds number plot of experimental data for all systems studied.

apparatus and the Graetz number for mass transfer.

It is important to note that in the calculation of the Graetz number the weight rate of flow was taken as the weight rate of flow of incoming dry gas and does not include the weight of vapor present after evaporation. Also, since the evaporation surface was a circle of diameter 1.05 cm., the integrated average length of path presented to the gas passing over the surface, $\pi D/4$, or 0.825 cm., was used in all calculations.

In the calculation of ϕ the vapor pressure of the liquid was taken at the liquid surface temperature, and consequently a calculated value of ϕ equal to unity corresponds to saturation in the exit gas at the surface temperature of the liquid and not at the exit gas temperature.

The ranges of variables covered are summarized in Table 2. The ratio p_{Bo}/p_{Bs} is the ratio of the partial pressure of inert component above the boundary layer to that at the surface, with the evaporating liquid assumed to exert its full vapor pressure in the surface layer. The horizontal approach velocity is calculated by dividing the volumetric rate of flow of inert gas through the system by the open cross section of the duct at the evaporating surface, that is the cross area of the tube minus the cross area of the projecting evaporator tube. The vapor velocity normal to the liquid surface was computed from the measured evaporation rate, the vapor density being evaluated at the surface temperature and vapor pressure.

Physical Properties

The diffusivity values used are from experimental literature tabulated by Wilke and Lee (*14*) or calculated from the equation of Hirschfelder, Bird, and Spotz (*4*). Corrections were made as needed for operating temperature and pressure.

System	D, sq. cm./sec. at 25°C., 1 atm.	Source
Air-water	0.260	Experimental
Air–carbon tetrachloride	0.0740	Calculated
Air-bromobenzene	0.0703	Calculated
Air-chlorobenzene	0.0747	Calculated
Helium-water	0.908	Experimental
Helium-chlorobenzene	0.329	Calculated

Viscosities for air, helium, and water vapor were taken from the literature (*6*); those for bromobenzene, chlorobenzene, carbon tetrachloride, and mixtures were calculated according to Bromley and Wilke (*1*). Vapor pressures for water, carbon tetrachloride, chlorobenzene, and bromobenzene are from the literature (*5, 8*).

Data Correlation

The data were calculated in terms of the analytical treatment of Butler and Plewes (*2*) for evaporation from one of two infinite parallel surfaces into a laminar air stream. The results for all systems studied are shown in Figure 5 and for individual systems in Figure 6 through 9. It is seen that the data of the present investigation are well correlated by the functional relation developed by Butler and Plewes; that is

$$\phi = 1 - 0.896e^{-2.43\psi} - 0.0609e^{-23.5\psi} - \cdots \quad (1)$$
$$(0 < 1/\psi < 10)$$

and

$$\phi = 1.47(1/\psi)^{-\frac{1}{2}} \qquad (1/\psi > 10) \quad (2)$$

where

$$\phi = \frac{y_v p_T}{p^*}$$

and

$$1/\psi = \frac{w}{\rho D_v x}$$

Equation (1) was derived on the assumption of a laminar velocity distribution between the two plates and is an infinite series converging only for $1/\psi$ less than 10. Butler and Plewes obtained Equation (2), applicable to higher values of $1/\psi$, by using a solution of Leveque (*7*) which is based on the assumption of a linear velocity gradient through a boundary layer in laminar flow between parallel plates. Both equations are two-dimensional solutions which neglect the effect of property differences

TABLE 2. RANGES OF VARIABLES COVERED

System	System pressure p_T, mm. Hg	Vapor pressure p^* mm. Hg	Dry-gas velocity u_0, cm./sec.	Diffusivity (operating condition) D_{12}, sq. cm./sec.	Reynolds number, N_{Re_x}	Graetz number, $1/\psi$	Schmidt number (surface)	Schmidt number (bulk)	v_n/u_0	p_{Bo}/p_{Bs}
Air-H_2O	20-700	9.9-23.3	0.161-58.2	0.280-9.50	0.155-153.	0.51-570	0.544-0.596	0.592-0.596	0.0877-17.8	1.03-2.37
Air-C_6H_5Cl	15-700	6.3-11.7	0.191-48.8	0.0810-3.77	0.072-134.	0.70-1,800	0.366-1.90	2.07-2.07	0.0388-12.6	1.01-2.75
Air-CCl_4	120-700	72.-112.	0.0129-52.1	0.0808-0.471	0.082-112.	0.76-1,440	0.272-1.08	2.07-2.07	0.0442-11.4	1.17-4.96
He-C_6H_5Cl	15-700	5.4-11.2	0.0625-27.0	0.356-16.3	0.006-2.4	0.12-52	0.105-2.45	3.74-3.74	0.370-19.4	1.02-2.17
Air-C_6H_5Br	15-100	3.5-4.0	0.369-12.2	0.537-3.54	0.098-24.	1.2-330	0.640-1.74	2.20-2.20	0.461-4.45	1.04-1.34
He-H_2O	35	10.2	15.4	19.0	0.5	4	0.483	1.35	1.96	1.49
All Systems	15-700	3.5-112.	0.0129-58.2	0.0808-19.0	0.006-153.	0.12-1,800	0.105-2.45	0.592-3.74	0.0388-19.4	1.01-4.96

in the direction normal to the evaporating surface. Schenck (*11*) obtained an equation practically identical with (1) for heat transfer from one of two infinite parallel plates to a gas in laminar flow.

Plewes, Butler, and Marshall (*9*) tested their theory with data on evapotion of solids from the bottom of a rectangular duct with data covering only the range of Equation (2), that is $1/\psi$ greater than 10. They found the slope of a log-log plot of ϕ vs. $1/\psi$ to be minus $\frac{2}{3}$, as predicted by Equation (2), but separate lines were obtained for each system studied.

In Figures 5 to 9 the dashed curves are calculated from Equation (1) and the solid lines (labeled Leveque) from Equation (2). The correlation of the present data is quite good, covering the wide range of evaporation rates, diffusivities, and other physical properties of the systems studied and the high ratio of partial pressures across the boundary layer. The diffusivities are often high in the present work because of the low pressures used.

It was not expected that the analysis of Butler and Plewes would apply to the data of this work, since their derivation was for the case of very dilute gas mixtures and for a constant stream velocity. A substantial part of the present data is for rich gas mixtures, and furthermore the evaporation increased the stream velocity severalfold in some cases. The agreement of the data with the Butler-Plewes and Leveque equations would appear to be fortuitous, and the very good correlation obtained must be considered to be empirical until shown otherwise.

In the Butler-Plewes treatment the evaporating surface is one of two parallel plates, whereas in the present work it is the flat open end of a vertical tube extending into a cylindrical horizontal glass duct. In this connection, however, it may be noted that the four points of the present investigation for evapotion of water from a nonprojecting surface into a stream of air in a square duct were also correlated in Figure 5 (shown as solid circles). It is surprising that the data for these dissimilar geometries follow the same correlation.

The data were also plotted with the conventional functions $N_{Sh} = F(N_{Re_x}, N_{Sc}, p_{Bm}/p_T)$ used. By analogy to the classical equation of Pohlhausen on heat transfer from a gas stream to a flat plate (*10*), the Sherwood number was assumed to be proportional to the one-third power of the Schmidt number. Correlation was improved somewhat by multiplying the Sherwood number by the first power of p_{Bm}/p_T (Figure 10).

For many of the experimental runs there was a very large difference between the Schmidt number at the upper edge of the boundary layer, calculated from the properties of the pure inert gas, and the Schmidt number at the evaporating surface, calculated for the properties at the composition and temperature of the surface layer. These differences result from high density gradients and appreciable viscosity differences through the boundary layer. In an extreme instance (run 186) the bulk Schmidt number was 3.74 and the surface Schmidt number 0.106, a ratio of 35 to 1. In such cases the use of an arithmetic average amounts to using practically one-half the larger number, and thus any effect of the surface conditions nearly drops out. In the absence of adequate theory there is little basis for a rational choice of the method of averaging to be used. In Figure 10 the geometric mean was arbitrarily chosen for the correlation in order to give weight to each end condition. Other methods of averaging, as well as other exponents such as 0.44 for the Schmidt number and 0.83 for the p_{Bm}/p_T ratio, could also be used with little effect on the scatter (*13*).

The data for the air-water and air-chlorobenzene systems (Figures 6 and 7) were quite good; for the air–carbon tetrachloride and helium-chlorobenzene systems (Figures 8 and 9) more scattering was in evidence. The reasons for this difference are, at least in part, experimental. In the helium runs flow control from the high-pressure tank was less steady. In the runs for air–carbon tetrachloride and helium-chlorobenzene the evaporation rates were much higher than for the other systems. This necessitated shorter time intervals between readings, leaving less time for careful measurements. There was a more rapid change in the position of the evaporating surface between readings, rendering measurement of surface temperature less accurate. Because the surface temperature fixes the vapor pressure and thus the driving force, the largest contribution of error to the experimental data is due to the temperature measurement rather than to the rate of evaporation measurement.

ACKNOWLEDGMENT

This investigation was carried out with financial support of the National Science Foundation. The University of North Dakota provided space, facilities, and equipment.

Dewey Wahl made the photographs of, and James Braus built the apparatus for, and obtained the data on, the square duct as senior thesis projects at the University of North Dakota.

NOTATION

D_v = diffusion coefficient for system carrier gas-evaporating substance, sq. ft./hr.
G = mass velocity of inert gas stream, lb./(hr.)(sq. ft.) of duct cross section.
K_g = mass transfer coefficient, lb. mole/hr. sq. ft. atm.
N_{Re_x} = length Reynolds number = $(xG)/\mu$
N_{Sc} = Schmidt number = $\mu/(\rho D_v)$
N_{Sh} = Sherwood number = $(K_g RTx)/D_v$
p^* = vapor pressure of evaporating liquid at T_s, atm.
p_{Bm} = mean partial pressure between p_{B0} and p_{Bs}, atm.
p_{B0} = partial pressure of carrier gas at leading edge, atm., = p_T.
p_{Bs} = partial pressure of carrier gas at surface, atm., = $p_T - p^*$
p_T = total pressure in system, atm.
R = gas constant, 0.729 (cu. ft.)(atm.)/(lb. mole)(°R.)
T = temperature, °R.
T_0 = bulk gas temperature, °R.
T_s = surface temperature, °R.
u_0 = average velocity of carrier gas approaching surface, ft./hr.
v_n = average normal velocity of vapor at surface, ft./hr.
w = carrier gas flow rate, lb./hr.
x = average length of evaporation surface, ft.
y_v = mole fraction of vapor in exit gas.

Greek Letters

μ = viscosity, lb./ft. hr.
ρ = density of gas, lb./cu. ft.
ϕ = $(y_v p_T)/p^*$ = fractional saturation of exit gas.
$1/\psi$ = $w/(\rho D_v x)$ = Graetz number for mass transfer.

LITERATURE CITED

1. Bromley, L. A., and C. R. Wilke, *Ind. Eng. Chem.*, **43**, 1641 (1951).
2. Butler, R. M., and A. C. Plewes, *Chem. Eng. Progr. Symposium Ser. No. 10*, **50**, 121 (1954).
3. Cairns, R. C., and G. H. Roper, *Chem. Eng. Sci.*, **3**, 97 (1954); **4**, 221 (1955).
4. Hirschfelder, J. O., R. B. Bird, and E. L. Spotz, *Chem. Revs.*, **44**, 205 (1949).
5. Lange, N. A., "Handbook of Chemistry," 5 ed., pp. 1422, 1443, Handbook Publishers, Sandusky, Ohio (1944).
6. *Ibid.*, p. 1588.
7. Leveque, J., *Ann. mines (12)*, **13**, 201, 305, 381 (1928).
8. Perry, J. H., ed., "Chemical Engineers' Handbook," 3 ed., p. 154, McGraw-Hill, New York (1950).
9. Plewes, A. C., R. M. Butler, and H. E. Marshall, *Chem. Eng. Progr.*, **50**, 77 (1954).
10. Pohlhausen, E., *Zeit. angew. Math. u. Mech.*, **1** (2), 115 (1921).
11. Schenck, J., *Appl. Sci. Research*, **A5**, 241 (1955).
12. Sherwood, T. K., and R. L. Pigford, "Absorption and Extraction," 2 ed., p. 67, McGraw-Hill, New York (*1952*).
13. Westkaemper, L. E., and R. R. White, *A. I. Ch.E. Journal*, **3**, 69 (1957).
14. Wilke, C. R., and C. Y. Lee, *Ind. Eng. Chem.*, **47**, 1253 (1955).

Manuscript received August 14, 1958; revision received November 24, 1958; paper accepted January 21, 1959.